Journal of Applied Mathematics and Computing (2022) 68:1545–1564
https://doi.org/10.1007/s12190-021-01571-4

ORIGINAL RESEARCH

A structure-preserving finite element discretization for the time-dependent Nernst-Planck equation

Qianru Zhang[1,2] · Bin Tu[3] · Qiaojun Fang[3,4,5] · Benzhuo Lu[1,2]

Received: 3 February 2021 / Revised: 14 May 2021 / Accepted: 6 June 2021 / Published online: 18 June 2021

Abstract
It is still a challenging task to get a satisfying numerical solution to the time-dependent Nernst-Planck (NP) equation, which satisfies the following three physical properties: solution nonnegativity, total mass conservation, and energy dissipation. In this work, we propose a structure-preserving finite element discretization for the time-dependent NP equation combining a reformulated Jordan-Kinderlehrer-Otto (JKO) scheme and Scharfetter-Gummel (SG) approximation. The JKO scheme transforms a partial differential equation solution problem into an optimization problem. Our finite element discretization strategy with the SG stabilization technique and the Fisher information regularization term in the reformulated JKO scheme can guarantee the convexity of the discrete objective function in the optimization problem. In this paper, we prove that our scheme can preserve discrete solution nonnegativity, maintain total mass conservation, and preserve the decay property of energy. These properties are all validated with our numerical experiments. Moreover, the later numerical results show that our scheme performs better than the traditional Galerkin method with linear Lagrangian basis functions in keeping the above physical properties even when the convection term is dominant and the grid is coarse.

Keywords Structure-preserving finite element discretization · Nernst-Planck equation · Scharfetter-Gummel approximation · Jordan-Kinderlehrer-Otto scheme

1 Introduction

The Nernst-Planck (NP) describes the motion of charged particles in different physical systems, such as biological ion channels [34,37], nanopores [36,41], and semiconduc-

✉ Bin Tu
tub@nanoctr.cn

✉ Benzhuo Lu
bzlu@lsec.cc.ac.cn

Extended author information available on the last page of the article

tor devices [2,4]. For a given bounded open domain $\Omega \subset \mathbb{R}^d$ $(d = 1, 2)$, we consider the time-dependent NP equation of the form

$$\begin{cases} \dfrac{\partial c}{\partial t} = -\nabla \cdot J = \nabla \cdot D(\nabla c + zc\nabla u), & \text{in } \Omega \times [0, T], \\ J \cdot \mathbf{n} = 0, & \text{on } \partial\Omega \times [0, T], \\ c(0, \cdot) = c^0, & \text{in } \Omega, \end{cases} \tag{1}$$

where $c(t, x)$ is the charged particle concentration function, $c^0(x)$ is an initial value of the concentration, and $u(x)$ is a drift potential. Constants z, $D > 0$ are the valence and diffusion coefficient of the charged particle.

Two salient properties can be directly obtained from the time-dependent NP Eq. (1): (i) the solution preserves nonnegative, and (ii) the total mass is maintained because of the zero flux condition across the boundary of the domain Ω. One more property of the NP equation is the energy dissipation. Referring to previous works [8,21,24,33], the NP equation can be regarded as a Wasserstein gradient flow concerning the energy $\mathcal{E}$ [1] defined on the space $\mathbb{P}(\Omega)$ of c (the concentration) which remains to be nonnegative with prescribed total mass:

$$\mathbb{P}(\Omega) = \{c \in L^1(\Omega) : \int_\Omega c(x) = \text{Constant}, c(x) \geq 0\},$$

namely $\mathcal{E} : \mathbb{P}(\Omega) \to \mathbb{R} \bigcup \{+\infty\}$. Correspondingly, the gradient of the energy is defined with the quadratic Wasserstein metric $\mathcal{W}_2$ as

$$\nabla_{\mathcal{W}_2} \mathcal{E}(c) = -\nabla \cdot (c \nabla \delta \mathcal{E}),$$

where δ refers to the first variation of c in this paper. The Wasserstein metric between two nonnegative measures $\rho^1, \rho^2 \in \mathbb{P}(\Omega)$ is defined as the cost of transporting one into the other in an optimal way, and it is obtained from the following optimization problem [21]

$$\mathcal{W}_2^2(\rho^1, \rho^2) = \inf_{\gamma \in \Gamma(\rho^1, \rho^2)} \int \int_{\Omega \times \Omega} |\mathbf{y} - \mathbf{x}|^2 d\gamma(\mathbf{x}, \mathbf{y}),$$

where $\Gamma(\rho^1, \rho^2)$ is the set of admissible transport plans on the space $\mathbb{P}(\Omega \times \Omega)$ with the first marginal ρ^1 and the second marginal ρ^2, and the symbol $|\cdot|$ denotes the usual Euclidean norm on $\mathbb{R}^d$. Then the first equation in (1) can be written as

$$\frac{\partial c}{\partial t} = -\nabla \cdot (cv) := \nabla \cdot [c \nabla (D \log c + Dzu)], \quad \text{in } \Omega \times [0, T].$$

Here, $v = -\nabla \delta \mathcal{E}$ is the velocity field and the definition of the energy is as follows

$$\mathcal{E}(c) = \int_\Omega (Dc \log c + Dzuc) dx.$$

The evolution of the energy along c is given by

$$\frac{d}{dt}\mathcal{E}(c)(t) = \int_\Omega \frac{\delta \mathcal{E}}{\delta c}\frac{\partial c}{\partial t}dx = -\int_\Omega |v(t,x)|^2 c(t,x)dx,$$

which means that the solution to (1) is the gradient flow of the steepest descent for the energy $\mathcal{E}$, and the energy related to the NP equation dissipates along the time.

The time-dependent NP equation is usually treated as a part of the time-dependent Poisson-Nernst-Planck (PNP) model, and several numerical methods with different properties for the PNP model have been constructed [3,14,17,29]. Most existing schemes [14,17,18] are specially designed to preserve total mass conservation or energy dissipation, and some of them [11,27,31] can further maintain nonnegativity of concentration when satisfying certain stability conditions. Currently, designing a numerical scheme that can preserve all three properties above at the discrete level is still a challenging problem [28–30,32]. The finite difference method in [29] can obtain positive solution with the explicit time discretization under a Courant-Friedrichs-Lewy (CFL) condition $\Delta t = O(\Delta x^2)$. But it needs to employ the semi-discrete scheme, in which time is continuous, to get the energy decay. A discontinuous Galerkin (DG) method [30] can dissipate the free energy, but an accuracy-preserving limiter is necessary for it to maintain solution positivity. To get the above three properties of the time-dependent PNP model well, the finite element scheme in [32] adopts the fully implicit backward Euler scheme, and the finite difference scheme in [28] employs the semi-implicit time discretization scheme. In this work, we propose a numerical method that can preserve these three properties just with the explicit time discretization scheme. And it is positivity-preserving for time steps of arbitrary size. In semiconductor device simulations, the NP equation usually serves as a convection-dominated problem, which makes most numerical schemes suffer from stability issues, and therefore, the solution positivity preservation fails. Many stabilization techniques [10,20,38,40] are proposed to prevent the spurious numerical oscillations. These methods can eliminate negative oscillations (negative concentration values) well, but they can also bring some spurious positive oscillations [19,20,22].

Currently, the optimal transport theory has been applied in the partial differential equation field [23,25,26], which provides a series of new efficient approaches for solving nonlinear evolution equations [6,13,33]. Besides the NP equation, many nonlinear evolution equations, such as the porous medium Eq. [33], total variation flows [7], quantum drifts [16], and heat evolutions on manifolds [12], can be interpreted as Wasserstein gradient flows, and the literature concerning this issue is steadily growing (see [1] and references therein). Thus, a new class of numerical schemes gradually develops based on the variational minimizing movement scheme — Jordan-Kinderlehrer-Otto (JKO) scheme following the seminal work by Jordan, Kinderlehrer, and Otto [21]. This scheme turns an evolution equation problem into an optimization problem, which is pretty different from the traditional Galerkin method. The JKO scheme provides a nonnegativity preserving, energy dissipating, and unconditionally stable time discretization. This scheme writes as

$$c^0 = c(0,x), \quad c^{k+1} = \arg\min_{c\in\mathbb{K}}\{\mathcal{W}_2^2(c,c^k) + 2\tau\mathcal{E}(c)\}, \quad k \geq 0,$$

where $\tau > 0$ is the time discretization step, $\mathbb{K} = \{c : c \in \mathbb{P}(\Omega),\ \int_\Omega c|x|^2 dx < +\infty\}$, and $\mathcal{W}_2$ is the Wasserstein distance between two nonnegative measures belonging to $\mathbb{P}(\Omega)$. In this work, we propose a structure-preserving finite element discretization for the time-dependent NP equation combining the reformulated JKO Scheme (2) [24]:

$$\begin{cases} c^{k+1}(x) = \arg\inf\limits_{c,m} \int_\Omega \left(\dfrac{||m(x)||^2}{c(x)} + \kappa^2\tau^2||\nabla \log c(x)||^2 c(x)\right)dx + 2\tau\mathcal{E}(c) \\ \qquad\qquad \text{s.t. } c(x) - c^k(x) + \nabla \cdot m(x) = 0,\ m \cdot \mathbf{n} = 0, \end{cases} \tag{2}$$

where $m = cv$, κ is the regularization parameter, and it is used to adjust the effect of the additional Fisher information regularization term $\int_\Omega ||\nabla \log c(x)||^2 c(x)dx$.

The finite element method (FEM for brevity) has been widely used in the solution of the NP equation [9,37,41], and it allows for easier modeling of complex geometrical and irregular shapes. Different types of boundary conditions can also be directly incorporated into this method. Moreover, the availability of a variety of finite element basis functions makes FEM a versatile and powerful numerical method. However, if the concentration is directly discretized with the linear Lagrangian basis functions, the discrete objective function in the reformulated JKO Scheme (2) is not smooth, and its global convexity can not be proved. Therefore, we employ the Scharfetter-Gummel (SG) approximation [35] in the spatial discretization of the reformulated JKO scheme, and the concentration is approximated with exponential basis functions on each edge of the element. The SG stabilization technique is first introduced in semiconductor simulations aiming at avoiding unphysical spurious oscillations near the boundary layers. In Theorem 1, we illustrate that our numerical scheme can preserve solution nonnegativity, total mass conservation, and energy dissipation, which is verified with later numerical experiments. And the numerical results show that our method performs better than the classical Galerkin method with linear Lagrangian basis functions, especially for convection-dominated NP equations and coarse grids. In the proof of Theorem 1, by referring to [24,26], we also present that our finite element discretization strategy and the additional Fisher information regularization term $\int_\Omega ||\nabla \log c(x)||^2 c(x)dx$ in (2) can guarantee the smoothness and convexity of the discrete objective function. Furthermore, the regularization term can automatically maintain nonnegativity of concentration. But it will polish the numerical solution and further affect the accuracy, therefore, choosing an appropriate regularization parameter κ is necessary for obtaining a satisfying numerical solution.

The rest of this paper is organized as follows. In Sect. 2, we construct a full discretization of the reformulated JKO method and study the properties of our numerical scheme. Then several numerical experiments are presented in Sect. 3 to validate theoretical properties of our scheme, and the paper is concluded in Sect. 4.

2 Full discretization of the reformulated JKO scheme

In this section, we will introduce the spatial discretization of the reformulated JKO scheme (2) in detail. And we shall prove that our finite element discretization for

the time-dependent NP Eq. (1) can guarantee the nonnegativity of discrete solutions, maintain total mass conservation, and preserve the decay property of energy.

To present our idea better, we will first establish the spatial discretization method on a one-dimensional computational region $[0, L]$ with a uniform grid $0 = x_{\frac{1}{2}} < x_{\frac{3}{2}} < \cdots < x_{N+\frac{1}{2}} = L$. For nonuniform grids, the corresponding spatial discretization scheme can be constructed similarly. On the uniform grid, we define

$$\begin{aligned} c_j^k &= c(t_k, x_j), \qquad 1 \le j \le N, \quad k \in \mathbb{N}^+; \\ m_{j+\frac{1}{2}}^k &= m(t_k, x_{j+\frac{1}{2}}), \qquad 0 \le j \le N, \quad k \in \mathbb{N}^+, \end{aligned}$$

where $x_j = j\Delta x$, $x_{j+\frac{1}{2}} = (j + \frac{1}{2})\Delta x$, $t_k = k\tau$, Δx is the space step, and $m_{\frac{1}{2}}^k = m_{N+\frac{1}{2}}^k = 0$ due to the Neumann boundary condition in (1).

We have tried to discretize the concentration c with the linear Lagrangian basis functions, but the obtained discrete objective function in (2) is not smooth, and its global convexity cannot be proved. Therefore, we introduce the SG approximation [35] into the spatial discretization of the reformulated JKO scheme. In the SG stabilization technique, the flux J and the electrical filed $E = -\nabla u$ are both regarded as constants over each egde $l_{ij} = \overline{x_i x_j}$, $j \in N(i)$, where $N(i)$ is the neighborhood of node i in the discretization grid. Then from the following two-point boundary value problem:

$$\begin{cases} \frac{dc}{dx} - zcE_{ij} = C_{ij}, \\ c(x_i) = c_i, \quad c(x_j) = c_j, \end{cases}$$

we can get the exponential fitting distribution of the concentration on the edge l_{ij}

$$c = (1 - g(x))c_i + g(x)c_j, \tag{3}$$

where the electrical field $E_{ij} = -\nabla u = \dfrac{u_i - u_j}{\Delta x}$, and the exponentially fitted SG function $g(x) = \dfrac{1 - \exp(z(u_i - u_j)\dfrac{x - x_i}{\Delta x})}{1 - \exp(z(u_i - u_j))}$. In this work, therefore, m is discretized with piecewise constant basis functions, and c is discretized with the above exponential basis functions (3). The discretization form of the objective function in (2) is as follows

$$\begin{aligned} F(\mathbf{m}, \mathbf{c}) &= \sum_{j=1}^{N-1} \frac{m_{j+\frac{1}{2}}^2 \Delta x}{c_{j+\frac{1}{2}}} + \kappa^2\tau^2 \sum_{j=1}^{N-1} \int_{x_j}^{x_{j+1}} (\frac{1}{c}\frac{dc}{dx})^2 c dx + 2\tau \sum_{j=1}^{N} D \int_{x_{j-\frac{1}{2}}}^{x_{j+\frac{1}{2}}} (c \log c + zuc) dx \\ &= \sum_{j=1}^{N-1} \left[\frac{m_{j+\frac{1}{2}}^2}{(c_{j+1} - c_j)g(x_{j+\frac{1}{2}}) + c_j} + \kappa^2\tau^2 \frac{(c_{j+1} - c_j)g'(x_{j+\frac{1}{2}})(\log c_{j+1} - \log c_j)}{\Delta x} \right] \Delta x \\ &\quad + 2\tau \sum_{j=1}^{N} D(c_j \log c_j + z u_j c_j)\Delta x. \end{aligned}$$

Here, $\mathbf{m} = (m_{\frac{1}{2}}, m_{\frac{3}{2}}, \cdots m_{N+\frac{1}{2}})$ and $\mathbf{c} = (c_1, c_2, \cdots c_N)$. We notice that $g(x_{j+\frac{1}{2}})$ and $g'(x_{j+\frac{1}{2}})$ have no definition when $u_j = u_{j+1}$. Then we redefine them referring to their respective limitations with $|u_j - u_{j+1}| \to 0$ as

$$g(x_{j+\frac{1}{2}}) = \begin{cases} \dfrac{1 - \exp(z(u_j - u_{j+1})\dfrac{x_{j+1/2} - x_j}{\Delta x})}{1 - \exp(z(u_j - u_{j+1}))}, & u_j \neq u_{j+1}, \\ \dfrac{x_{j+1/2} - x_j}{\Delta x}, & u_j = u_{j+1} \end{cases}$$

$$g'(x_{j+\frac{1}{2}}) = \begin{cases} \dfrac{\exp(z(u_j - u_{j+1})\dfrac{x_{j+1/2} - x_j}{\Delta x})}{1 - \exp(z(u_j - u_{j+1}))} \dfrac{z(u_{j+1} - u_j)}{\Delta x}, & u_j \neq u_{j+1}, \\ \dfrac{1}{\Delta x}, & u_j = u_{j+1}. \end{cases}$$

By integrating the constraint of (2) on each interval $[x_{j-\frac{1}{2}}, x_{j+\frac{1}{2}}]$ and using the integration by parts, we get the spatial discretization of it as follows

$$c_j - c_j^k + \frac{1}{\Delta x}(m_{j+\frac{1}{2}} - m_{j-\frac{1}{2}}) = 0, \quad 1 \le j \le N.$$

The above spatial discretization method can be extended to a two-dimension situation directly. On a two-dimensional computational region $[0, L]^2$ with a uniform grid $0 = x_{\frac{1}{2}} < x_{\frac{3}{2}} < \cdots < x_{N_x+\frac{1}{2}} = L$ and $0 = y_{\frac{1}{2}} < y_{\frac{3}{2}} < \cdots < y_{N_y+\frac{1}{2}} = L$, we define

$$\begin{aligned} c_{j,l}^k &= c(t_k, x_j, y_l), && 1 \le j \le N_x, \quad 1 \le l \le N_y, \quad k \in \mathbb{N}^+; \\ m_{j+\frac{1}{2},l}^k &= m_x(t_k, x_{j+\frac{1}{2}}, y_l), && 0 \le j \le N_x, \quad 1 \le l \le N_y, \quad k \in \mathbb{N}^+; \\ m_{j,l+\frac{1}{2}}^k &= m_y(t_k, x_j, y_{l+\frac{1}{2}}), && 1 \le j \le N_x, \quad 0 \le l \le N_y, \quad k \in \mathbb{N}^+. \end{aligned}$$

Here, $x_j = j\Delta x$, $x_{j+\frac{1}{2}} = (j + \frac{1}{2})\Delta x$, $y_l = l\Delta y$, $y_{l+\frac{1}{2}} = (l + \frac{1}{2})\Delta y$, Δx and Δy are the space steps along different coordinate axes. The zero-flux Neumann boundary condition in (1) is imposed dimension by dimension, that is

$$\begin{aligned} m_{\frac{1}{2},l}^k &= m_{N_x+\frac{1}{2},l}^k = 0, && 1 \le l \le N_y, \quad k \in \mathbb{N}^+; \\ m_{j,\frac{1}{2}}^k &= m_{j,N_y+\frac{1}{2}}^k = 0, && 1 \le j \le N_x, \quad k \in \mathbb{N}^+. \end{aligned}$$

The exponential fitting distributions of the concentration on edges $\overline{x_{j,l}x_{j+1,l}}$ and $\overline{x_{j,l}x_{j,l+1}}$ are respectively written as

$$\begin{aligned} c(x, y_l) &= (1 - g(x, y_l))c_{j,l} + g(x, y_l)c_{j+1,l}, \\ c(x_j, y) &= (1 - g(x_j, y))c_{j,l} + g(x_j, y)c_{j,l+1}, \end{aligned} \tag{4}$$

$$g(x, y_l) = \frac{1 - \exp(z(u_{j,l} - u_{j+1,l})\dfrac{x - x_j}{\Delta x})}{1 - \exp(z(u_{j,l} - u_{j+1,l}))},$$
$$g(x_j, y) = \frac{1 - \exp(z(u_{j,l} - u_{j,l+1})\dfrac{y - y_l}{\Delta y})}{1 - \exp(z(u_{j,l} - u_{j,l+1}))}. \tag{5}$$

Similar to the one-dimensional case, on each edge of the discrete grid, m_x and m_y are discretized with piecewise constant basis functions, and c is discretized with the corresponding exponential basis functions (4) and (5). Then the discrete form of the objective function in (2) writes as

$$\begin{aligned}
&F(\mathbf{m}, \mathbf{c}) \\
&= \sum_{l=1}^{N_y} \sum_{j=1}^{N_x - 1} \left[\frac{m_{j+\frac{1}{2},l}^2}{c_{j,l} + g_{j+\frac{1}{2},l}(c_{j+1,l} - c_{j,l})} + \frac{\kappa^2 \tau^2}{\Delta x}(c_{j+1,l} - c_{j,l}) g'_{j+\frac{1}{2},l}(\log c_{j+1,l} - \log c_{j,l}) \right] \Delta x \Delta y \\
&+ \sum_{j=1}^{N_x} \sum_{l=1}^{N_y - 1} \left[\frac{m_{j,l+\frac{1}{2}}^2}{c_{j,l} + g_{j,l+\frac{1}{2}}(c_{j,l+1} - c_{j,l})} + \frac{\kappa^2 \tau^2}{\Delta y}(c_{j,l+1} - c_{j,l}) g'_{j,l+\frac{1}{2}}(\log c_{j,l+1} - \log c_{j,l}) \right] \Delta x \Delta y \\
&+ 2\tau \sum_{j=1}^{N_x} \sum_{l=1}^{N_y} D(c_{j,l} \log c_{j,l} + z u_{j,l} c_{j,l}) \Delta x \Delta y,
\end{aligned}$$

and the corresponding constraint in (2) becomes

$$c_{j,l} - c_{j,l}^k + \frac{m_{j+\frac{1}{2},l} - m_{j-\frac{1}{2},l}}{\Delta x} + \frac{m_{j,l+\frac{1}{2}} - m_{j,l-\frac{1}{2}}}{\Delta y} = 0,$$
$$1 \le j \le N_x,\ 1 \le l \le N_y.$$

Here, $\mathbf{m} = (\mathbf{m}_x, \mathbf{m}_y)$, $\mathbf{m}_x = (m_{1+\frac{1}{2},1}, \cdots, m_{1+\frac{1}{2},N_y}, \cdots, m_{N_x-\frac{1}{2},1}, \cdots, m_{N_x-\frac{1}{2},N_y})$, $\mathbf{m}_y = (m_{1,1+\frac{1}{2}}, \cdots, m_{1,N_y-\frac{1}{2}}, \cdots, m_{N_x,1+\frac{1}{2}}, \cdots, m_{N_x,N_y-\frac{1}{2}})$, and $\mathbf{c} = (c_{1,1}, \cdots, c_{1,N_y}, \cdots, c_{N_x,1}, \cdots, c_{N_x,N_y})$. When the potential of two adjacent points are equal, we also need to redefine $g(x, y)$ and its gradient as follows,

$$g_{j+\frac{1}{2},l} = g(x_{j+\frac{1}{2}}, y_l) = \begin{cases} \dfrac{1 - \exp\left(z(u_{j,l} - u_{j+1,l})\dfrac{x_{j+\frac{1}{2}} - x_j}{\Delta x}\right)}{1 - \exp(z(u_{j,l} - u_{j+1,l}))}, & u_{j,l} \ne u_{j+1,l} \\ \dfrac{x_{j+\frac{1}{2}} - x_j}{\Delta x}, & u_{j,l} = u_{j+1,l}; \end{cases}$$

$$g'_{j+\frac{1}{2},l} = g'_x(x_{j+\frac{1}{2}}, y_l) = \begin{cases} \dfrac{\exp\left(z(u_{j,l} - u_{j+1,l})\dfrac{x_{j+\frac{1}{2}} - x_j}{\Delta x}\right)}{1 - \exp(z(u_{j,l} - u_{j+1,l}))} \dfrac{z(u_{j+1,l} - u_{j,l})}{\Delta x}, & u_{j,l} \ne u_{j+1,l}, \\ \dfrac{1}{\Delta x}, & u_{j,l} = u_{j+1,l}; \end{cases}$$

$$g_{j,l+\frac{1}{2}} = g(x_j, y_{l+\frac{1}{2}}) = \begin{cases} \dfrac{1-\exp\left(z(u_{j,l}-u_{j,l+1})\dfrac{y_{l+\frac{1}{2}}-y_l}{\Delta y}\right)}{1-\exp(z(u_{j,l}-u_{j,l+1}))}, & u_{j,l} \neq u_{j,l+1}, \\ \dfrac{y_{l+\frac{1}{2}}-y_l}{\Delta y}, & u_{j,l} = u_{j,l+l}; \end{cases}$$

$$g'_{j,l+\frac{1}{2}} = g'_y(x_j, y_{l+\frac{1}{2}}) = \begin{cases} \dfrac{\exp\left(z(u_{j,l}-u_{j,l+1})\dfrac{y_{l+\frac{1}{2}}-y_l}{\Delta y}\right)}{1-\exp(z(u_{j,l}-u_{j,l+1}))}\dfrac{z(u_{j,l+1}-u_{j,l})}{\Delta y}, & u_{j,l} \neq u_{j,l+1}, \\ \dfrac{1}{\Delta y}, & u_{j,l} = u_{j,l+1}. \end{cases}$$

According to the above spatial discretization, we get a concise full discretization of the reformulated JKO Scheme (2):

$$\begin{cases} \mathbf{c}^{k+1} = \min\limits_{\mathbf{c}\geq 0, \mathbf{m}} F(\mathbf{m}, \mathbf{c}) \\ \quad = \sum\limits_{\mathbf{i}\in V}\left[\dfrac{m^2_{\mathbf{i}+\frac{1}{2}\mathbf{e_i}}}{c_{\mathbf{i}}+g_{\mathbf{i}+\frac{1}{2}\mathbf{e_i}}(c_{\mathbf{i}+\mathbf{e_i}}-c_{\mathbf{i}})}+\dfrac{\kappa^2\tau^2}{\mathbf{\Delta x_i}}(c_{\mathbf{i}+\mathbf{e_i}}-c_{\mathbf{i}})g'_{\mathbf{i}+\frac{1}{2}\mathbf{e}}(\log c_{\mathbf{i}+\mathbf{e_i}}-\log c_{\mathbf{i}})\right]\mathbf{\Delta x} \\ \quad + 2\tau\sum\limits_{\mathbf{i}\in V} D(c_{\mathbf{i}}\log c_{\mathbf{i}}+zu_{\mathbf{i}}c_{\mathbf{i}})\mathbf{\Delta x} \\ \quad s.t. \quad c_{\mathbf{i}}-c^k_{\mathbf{i}}+\sum\limits_{\mathbf{e_i}}\dfrac{m_{\mathbf{i}+\frac{1}{2}\mathbf{e_i}}-m_{\mathbf{i}-\frac{1}{2}\mathbf{e_i}}}{\mathbf{\Delta x_i}}=0, \quad \mathbf{i}\in V. \end{cases} \tag{6}$$

Here, $\mathbf{i} = (j, l)$, $\mathbf{\Delta x_i} = \Delta x$ or Δy, and $\mathbf{\Delta x} = \prod_{\mathbf{i}} \mathbf{\Delta x}_i$, V is the vertices set of the discrete grid. On nonuniform grids, the corresponding full discretization can be derived similarly.

The additional constraints $c_{\mathbf{i}} \geq 0,\ \forall\, \mathbf{i} \in V$ of the above optimization problem (6) aiming to avoid unexpected negative solution values when this optimization problem does not fully converge. Next we will prove several properties of our numerical method (6).

Theorem 1 *Assume that the total mass of initial values of the concentration is positive, i.e.* $\sum_{\mathbf{i}\in V} c^0_{\mathbf{i}} > 0$. *The time discretization step* τ *and the regularization parameter* κ *are assumed to be larger than zero. For any* $k \geq 0$, *the following properties hold for our method (6):*

(i) The optimization problem (6) has a unique minimizer $\mathbf{c}^{k+1}$ *;*

(ii) Use $\mathcal{A}(\mathbf{c})$ *to denote the regularization term*

$$\mathcal{A}(\mathbf{c}) = \sum_{\mathbf{i}\in V}\frac{(c_{\mathbf{i}+\mathbf{e_i}}-c_{\mathbf{i}})g'_{\mathbf{i}+\frac{1}{2}\mathbf{e_i}}(\log c_{\mathbf{i}+\mathbf{e_i}}-\log c_{\mathbf{i}})}{\mathbf{\Delta x_i}},$$

and the modified energy decays

$$\frac{\kappa^2\tau}{2}\mathcal{A}(\mathbf{c}^{k+1})+\mathcal{E}(\mathbf{c}^{k+1}) \leq \frac{\kappa^2\tau}{2}\mathcal{A}(\mathbf{c}^k)+\mathcal{E}(\mathbf{c}^k);$$

(iii) The concentration positivity is preserved

$$c_{\mathbf{i}}^{k+1} > 0, \quad \forall\, \mathbf{i} \in V;$$

(iv) The total mass conservation is maintained

$$\sum_{\mathbf{i}\in V} c_{\mathbf{i}}^{k+1} = \sum_{\mathbf{i}\in V} c_{\mathbf{i}}^{0};$$

Proof Firstly, we prove (iv) is true, that is the total mass conservation is maintained. From the constraint in (6), we have

$$\sum_{\mathbf{i}\in V}(c_{\mathbf{i}}^{k+1} - c_{\mathbf{i}}^{k}) = -\sum_{\mathbf{i}\in V}\sum_{\mathbf{e_i}} \frac{1}{\mathbf{\Delta x_i}}(m_{\mathbf{i}+\frac{1}{2}\mathbf{e_i}} - m_{\mathbf{i}-\frac{1}{2}\mathbf{e_i}}) = 0,$$

which illustrates that $\sum_{\mathbf{i}\in V} c_{\mathbf{i}}^{k+1} = \sum_{\mathbf{i}\in V} c_{\mathbf{i}}^{0} > 0$, $\forall k \geq 1$.

Then we shall show (iii) is true, that is the minimizer of (6) with regard to $\mathbf{c}$ is positive. This is true because

$$\lim_{\min_{\mathbf{i}\in V} c_{\mathbf{i}} \to 0} \mathcal{A}(\mathbf{c}) = +\infty. \tag{7}$$

Suppose (7) is not true, then there exist some $c_{\mathbf{i}^*} = 0,\ \mathbf{i}^* \in V$, such that

$$C \geq \mathcal{A}(c) = \sum_{\mathbf{i}\in V} \frac{(c_{\mathbf{i}+\mathbf{e_i}} - c_{\mathbf{i}})g'_{\mathbf{i}+\frac{1}{2}\mathbf{e_i}}(\log c_{\mathbf{i}+\mathbf{e_i}} - \log c_{\mathbf{i}})}{\mathbf{\Delta x_i}}, \tag{8}$$

C is a positive constant. Notice that every term in (8) is nonnegative, then

$$+\infty > C \geq (c_{\mathbf{i}} - c_{\mathbf{i_n}})g'_{\frac{\mathbf{i}+\mathbf{i_n}}{2}}(\log c_{\mathbf{i}} - \log c_{\mathbf{i_n}}),\ \forall\, \mathbf{i} \in V,\ \mathbf{i_n} \in N(\mathbf{i}),$$

where $N(\mathbf{i})$ is the neighbour node set of node $\mathbf{i}$ in the discretization grid. This implies that for any $\bar{\mathbf{i}} \in N(\mathbf{i}^*)$, $c_{\bar{\mathbf{i}}} = 0$, when $c_{\mathbf{i}^*} = 0$. Otherwise, there exists $\bar{\mathbf{i}} \in N(\mathbf{i}^*)$, $c_{\bar{\mathbf{i}}} \neq 0$, we have

$$\begin{aligned}&\lim_{c_{\mathbf{i}^*}\to 0}(c_{\bar{\mathbf{i}}} - c_{\mathbf{i}^*})g'_{\frac{\mathbf{i}^*+\bar{\mathbf{i}}}{2}}(\log c_{\bar{\mathbf{i}}} - \log c_{\mathbf{i}^*})\\ &= \lim_{c_{\mathbf{i}^*}\to 0}(c_{\bar{\mathbf{i}}})g'_{\frac{\mathbf{i}^*+\bar{\mathbf{i}}}{2}}(\log c_{\bar{\mathbf{i}}} - \log c_{\mathbf{i}^*}) = +\infty.\end{aligned}$$

Similarly, for any $\bar{\bar{\mathbf{i}}} \in N(\bar{\mathbf{i}})$, we can get $c_{\bar{\bar{\mathbf{i}}}} = 0$. After finite step iterations, we obtain $c_{\mathbf{i}} = 0, \forall\, \mathbf{i} \in V$ which contradicts $\sum_{\mathbf{i}\in V} c_{\mathbf{i}} = \sum_{\mathbf{i}\in V} c_{\mathbf{i}}^{0} > 0$.

Next, we prove that (i) is true. For notational convenience, we denote

$$\mathcal{B}(\mathbf{m}, \mathbf{c}) = \sum_{\mathbf{i}\in V} \frac{m_{\mathbf{i}+\frac{1}{2}\mathbf{e_i}}^2}{c_{\mathbf{i}} + g_{\mathbf{i}+\frac{1}{2}\mathbf{e_i}}(c_{\mathbf{i}+\mathbf{e_i}} - c_{\mathbf{i}})}.$$

We need to show that $\mathcal{B}(\mathbf{m}, \mathbf{c}) + \kappa^2\tau^2\mathcal{A}(\mathbf{c})$ is strictly convex in $(\mathbf{m}, \mathbf{c})$ with constraints $\sum_{\mathbf{i}\in V} c_{\mathbf{i}} = \sum_{\mathbf{i}\in V} c_{\mathbf{i}}^0$ and $c_{\mathbf{i}} > 0, \forall\, \mathbf{i} \in V$. We first prove that $\mathcal{A}(\mathbf{c})$ is strictly convex. Notice the fact

$$(\mathcal{A}_{\mathbf{cc}})_{\mathbf{i},\mathbf{i_j}} = \frac{\partial^2\mathcal{A}(\mathbf{c})}{\partial c_{\mathbf{i}}\partial c_{\mathbf{i_j}}} = \begin{cases} -\dfrac{1}{c_{\mathbf{i}}c_{\mathbf{i_j}}} t_{\mathbf{i},\mathbf{i_j}}, & \text{if } \mathbf{i_j} \in N(\mathbf{i}), \\ \dfrac{1}{c_{\mathbf{i}}^2} \displaystyle\sum_{\mathbf{i_k}\in N(\mathbf{i})} t_{\mathbf{i},\mathbf{i_k}}, & \text{if } \mathbf{i_j} = \mathbf{i}, \\ 0, & \text{otherwise}, \end{cases}$$

where $t_{\mathbf{i},\mathbf{i_j}} = \frac{1}{\Delta \mathbf{x_i}}(c_{\mathbf{i}} + c_{\mathbf{i_j}})g'_{\frac{\mathbf{i}+\mathbf{i_j}}{2}} > 0$. Therefore, for any unit vector $\boldsymbol{\sigma}$ satisfying $\sum_{\mathbf{i}\in V} \sigma_{\mathbf{i}} = 0$, which is related to the constraint $\sum_{\mathbf{i}\in V} c_{\mathbf{i}} = \sum_{\mathbf{i}\in V} c_{\mathbf{i}}^0$, we have

$$\begin{aligned} \boldsymbol{\sigma}^T\mathcal{A}_{\mathbf{cc}}\boldsymbol{\sigma} &= \frac{1}{2}\sum_{(\mathbf{i},\mathbf{i_j})\in E}\left(\frac{\sigma_{\mathbf{i}}^2}{c_{\mathbf{i}}^2} + \frac{\sigma_{\mathbf{i_j}}^2}{c_{\mathbf{i_j}}^2} - 2\frac{\sigma_{\mathbf{i}}\sigma_{\mathbf{i_j}}}{c_{\mathbf{i}}c_{\mathbf{i_j}}}\right)t_{\mathbf{i},\mathbf{i_j}} \\ &= \frac{1}{2}\sum_{(\mathbf{i},\mathbf{i_j})\in E}\left(\frac{\sigma_{\mathbf{i}}^2}{c_{\mathbf{i}}^2} - \frac{\sigma_{\mathbf{i_j}}^2}{c_{\mathbf{i_j}}^2}\right)^2 t_{\mathbf{i},\mathbf{i_j}} \geq 0. \end{aligned} \tag{9}$$

Here, E is the edge set of the discrete grid. In fact, the inequality in (9) is strict, that is

$$\boldsymbol{\sigma}^T\mathcal{A}_{cc}\boldsymbol{\sigma} > 0. \tag{10}$$

If (10) is not true, there exists a unit vector $\boldsymbol{\sigma}^*$ with $\sum_{\mathbf{i}\in V}\sigma_{\mathbf{i}}^* = 0$ such that

$$\boldsymbol{\sigma}^{*T}\mathcal{A}_{\mathbf{cc}}\boldsymbol{\sigma}^* = \frac{1}{2}\sum_{(\mathbf{i},\mathbf{i_j})\in E}\left(\frac{\sigma_{\mathbf{i}}^2}{c_{\mathbf{i}}^2} - \frac{\sigma_{\mathbf{i_j}}^2}{c_{\mathbf{i_j}}^2}\right)^2 t_{\mathbf{i},\mathbf{i_j}} = 0,$$

then $\dfrac{\sigma_1^*}{c_1} = \dfrac{\sigma_2^*}{c_2} = \cdots = \dfrac{\sigma_{|V|}^*}{c_{|V|}}$. From the constraint $\sum_{\mathbf{i}\in V}\sigma_{\mathbf{i}}^* = 0$, we get $\sigma_1^* = \sigma_2^* = \cdots = \sigma_{|V|}^* = 0$, which contradicts the assumption that $\boldsymbol{\sigma}^*$ is a unit vector.

Secondly, we prove that $\mathcal{B}(\mathbf{m}, \mathbf{c}) + \kappa^2\tau^2\mathcal{A}(\mathbf{c})$ is strictly convex. Referring to the constraints of $\mathbf{c}$, we notice that this objective function is smooth. Therefore, we only need to show that the following inequality (11) holds,

$$\mathcal{Q}(\mathbf{h}, \boldsymbol{\sigma}) = \begin{pmatrix}\mathbf{h}\\ \boldsymbol{\sigma}\end{pmatrix}^T \begin{pmatrix}\mathcal{B}_{\mathbf{mm}} & \mathcal{B}_{\mathbf{mc}}\\ \mathcal{B}_{\mathbf{cm}} & \mathcal{B}_{\mathbf{cc}}\end{pmatrix}\begin{pmatrix}\mathbf{h}\\ \boldsymbol{\sigma}\end{pmatrix} + \kappa^2\tau^2\boldsymbol{\sigma}^T\mathcal{A}_{\mathbf{cc}}\boldsymbol{\sigma} > 0, \tag{11}$$

where

$$\mathbf{h} \in \mathbb{R}^{|E|}, \quad \boldsymbol{\sigma} \in \mathbb{R}^{|V|}, \quad \mathbf{h}^T\mathbf{h} + \boldsymbol{\sigma}^T\boldsymbol{\sigma} = 1, \quad \sum_{\mathbf{i}\in V} \sigma_{\mathbf{i}} = 0.$$

Because $(c_{\mathbf{i}+\mathbf{e_i}} - c_{\mathbf{i}})g_{\mathbf{i}+\frac{1}{2}\mathbf{e_i}} + c_{\mathbf{i}} > 0$ and $\frac{m^2_{\mathbf{i}+\frac{1}{2}\mathbf{e_i}}}{(c_{\mathbf{i}+\mathbf{e_i}}-c_{\mathbf{i}})g_{\mathbf{i}+\frac{1}{2}\mathbf{e_i}}+c_{\mathbf{i}}}$ is concave on variables $c_{\mathbf{i}}$ and $c_{\mathbf{i}+\mathbf{e_i}}$, $\mathcal{B}(\mathbf{m}, \mathbf{c})$ is convex. Then we get

$$\mathcal{Q}(\mathbf{h}, \boldsymbol{\sigma}) = \begin{pmatrix}\mathbf{h}\\ \boldsymbol{\sigma}\end{pmatrix}^T \begin{pmatrix}\mathcal{B}_{\mathbf{mm}} & \mathcal{B}_{\mathbf{mc}}\\ \mathcal{B}_{\mathbf{cm}} & \mathcal{B}_{\mathbf{cc}}\end{pmatrix} \begin{pmatrix}\mathbf{h}\\ \boldsymbol{\sigma}\end{pmatrix} + \kappa^2\tau^2\boldsymbol{\sigma}^T\mathcal{A}_{\mathbf{cc}}\boldsymbol{\sigma} \geq 0,$$

and the inequality in it is also strict. Suppose there exists $(\mathbf{h}^*, \boldsymbol{\sigma}^*)$ satisfying

$$\mathcal{Q}(\mathbf{h}^*, \boldsymbol{\sigma}^*) = 0,$$

then $\sigma^* = 0$ referring to (10) and $\mathbf{h}^{*T}\mathcal{B}_{\mathbf{mm}}\mathbf{h}^* = 0$. Since

$$\mathcal{B}_{\mathbf{mm}} = \mathrm{diag}\Big(\frac{2}{(c_{\mathbf{i}+\mathbf{e_i}} - c_{\mathbf{i}})g_{\mathbf{i}+\frac{1}{2}\mathbf{e_i}} + c_{\mathbf{i}}}\Big)_{\mathbf{i}+\frac{1}{2}\mathbf{e_i}\in E}$$

is positive definite, we have $\mathbf{h}^* = 0$, which contradicts the constraint $\mathbf{h}^T\mathbf{h} + \boldsymbol{\sigma}^T\boldsymbol{\sigma} = 1$. Based on the above statements, we illustrate that there is a unique solution $\mathbf{c}^{k+1}$ for the optimization problem (6).

At last, we prove (ii) is true. Use $(\mathbf{m}^{k+1}, \mathbf{c}^{k+1})$ to denote the minimizer of the problem (6), we can get

$$F(\mathbf{m}^{k+1}, \mathbf{c}^{k+1}) \leq F(\mathbf{0}, \mathbf{c}^k),$$

which implies

$$\begin{aligned}\kappa^2\tau^2\mathcal{A}(\mathbf{c}^{k+1}) + 2\tau\mathcal{E}(\mathbf{c}^{k+1}) &\leq \mathcal{B}(\mathbf{m}^{k+1}, \mathbf{c}^{k+1}) + \kappa^2\tau^2\mathcal{A}(\mathbf{c}^{k+1}) + 2\tau\mathcal{E}(\mathbf{c}^{k+1})\\ &\leq \kappa^2\tau^2\mathcal{A}(\mathbf{c}^k) + 2\tau\mathcal{E}(\mathbf{c}^k).\end{aligned}$$

This is end of the whole proof. □

In this paper, the optimization problem (6) is solved with an open-source software package, Ipopt (Interior Point Optimizer) [39]. We choose a limited-memory quasi-Newton method to approximate the Hessian of the Lagrangian, and the convergence tolerance of the interior point line search filter algorithm is set to be 10^{-8}.

3 Numerical experiments

In this section, we perform some numerical experiments to verify that our finite element scheme (6) can preserve solution nonnegativity, energy dissipation, and total

Table 1 Time convergence order of our scheme with $t_{max} = 0.5$

τ	0.25	0.125	0.0625	0.03125	0.015625	0.0078125	0.00390625
ϵ_τ	0.1885	0.0766	0.0316	0.0137	0.0063	0.0030	0.0015
order	/	1.2992	1.2789	1.2052	1.1269	1.0635	1.0427

mass conservation ignoring rounding errors. For simplicity, in the following numerical examples, we always let $D = 1$ and $z = 1$. On a discrete grid, the energy $\mathcal{E}(\mathbf{c})$ is calculated as

$$\mathcal{E}(\mathbf{c}) = \sum_{\mathbf{i}\in V} D(c_{\mathbf{i}} \log c_{\mathbf{i}} + z u_{\mathbf{i}} c_{\mathbf{i}}) \mathbf{\Delta x}. \tag{12}$$

Referring to [5], a unique equilibrium solution of the NP Eq. (1) with the corresponding initial condition can be defined on a discrete grid as

$$c_{\mathbf{i}}^{\infty} = M \exp(-z u_{\mathbf{i}}), \quad \mathbf{i} \in V,$$

where $M = \frac{\sum_{\mathbf{i}\in V} c_{\mathbf{i}}^0 \mathbf{\Delta x}}{\sum_{\mathbf{i}\in V} \exp(-z u_{\mathbf{i}}) \mathbf{\Delta x}}$. Thus the steady state energy $\mathcal{E}_\infty$ writes as

$$\mathcal{E}_\infty = \sum_{\mathbf{i}\in V} D(c_{\mathbf{i}}^{\infty} \log c_{\mathbf{i}}^{\infty} + z u_{\mathbf{i}} c_{\mathbf{i}}^{\infty}) \mathbf{\Delta x}.$$

Example 1 For a specific drift potential $u(x) = -hx$, there exists an analytical solution for the NP Eq. (1) on the computational region $[0, 1] \times [0, T]$:

$$c(t, x) = \exp(-\alpha t + \frac{h}{2} x)(\pi \cos(\pi x) + \frac{h}{2} \sin(\pi x)) + \pi \exp(h(x - \frac{1}{2})),$$
$$x \in [0, 1], \ t \in [0, T],$$

where $\alpha = \pi^2 + \frac{h^2}{4}$, and h is the parameter designed to control the strength of the convection term of the NP Eq. (1).

Case 1

In this case, we let $h = 1$ and use this analytical solution to check the accuracy of our scheme. Firstly, we choose a small space step $\Delta x = 0.002$ and let $\kappa = 0$. The error concerning the time step is defined as follows

$$\epsilon_\tau = \|c_\tau(t_{max}, \cdot) - c(t_{max}, \cdot)\|_{l_1} = \sum_{j=1}^{N} |(c_\tau)_j(t_{max}) - (c)_j(t_{max})| \Delta x.$$

Table 1 illustrates that the time discretization in our scheme is first-order accurate, which coincides with Theorem 3 in [24].

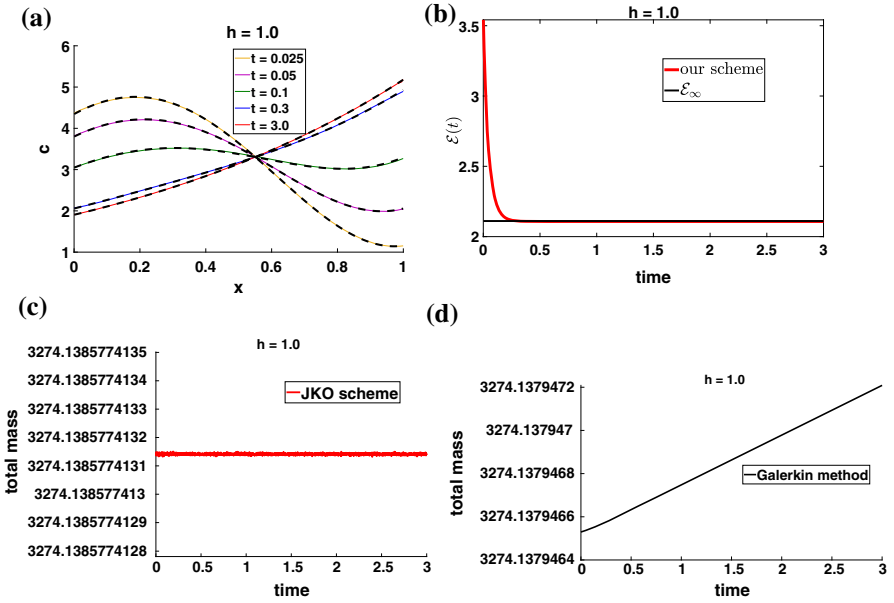

Fig. 1 **a** Evolution of the concentration $c(x, t)$(see black dash curves for respective exact solution), **b** energy dissipation, **c** total mass calculated with our scheme, and **d** total mass obtained from the Galerkin method over the time interval $[0, T]$ with $T = 3$, $\Delta x = 0.001$, $\tau = 0.001$, $\kappa = 0$

Then we plot the evolution of the concentration $c(t, x)$ over time in Fig. 1a, which shows that the numerical solution is in good agreement with the analytic solution. In Fig. 1b, it is seen that the energy dissipates along the time, and it finally reaches to the steady state $\mathcal{E}_\infty$. And Fig. 1c illustrates that the total mass conservation can be maintained, ignoring rounding errors. The total mass fluctuations are always less than 10^{-10}. The classical Galerkin method with linear Lagrangian basis functions is also applied to this case, and Fig. 1d illustrates that the classical Galerkin method has a poor performance in maintaining the total mass conservation, which has been mentioned in [15]. Then, [15] adopts the Raviart-Thomas (RT) mixed FEM to locally preserve the mass conservation, which is one of its attractive features over the conventional Lagrange FEMs.

Case 2

In this case, we let $h = 10.0$ and make a comparison between the classical Galerkin method and our scheme on a relatively coarse grid in space, $\Delta x = 0.25$. Fig. 2 shows that the Galerkin method may suffer from stability problems and produce large negative oscillations (negative concentration values) on coarse grids. Our scheme can eliminate negative oscillations and always preserve the solution nonnegativity, although the numerical solution is not in good agreement with the analytical solution on the same coarse grid. In Fig. 3, we examine the effect of the regularization parameter κ through comparing numerical solutions calculated by our scheme with different κ. It is observed that the numerical solution becomes smoother as κ increases, which illustrates that the regularization term will polish the numerical solution and further

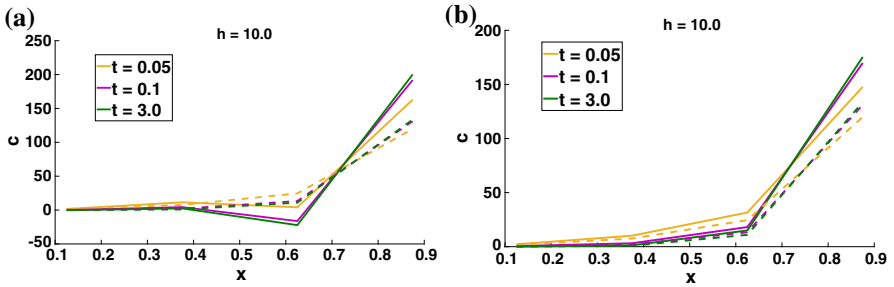

Fig. 2 Evolution of the concentration $c(x, t)$(see dash curves for respective exact solutions) with $T = 3$, $\Delta x = 0.25$, $\tau = 0.001$, and $\kappa^2 = 0.5$ using two methods: **a** the Galerkin method, **b** our scheme

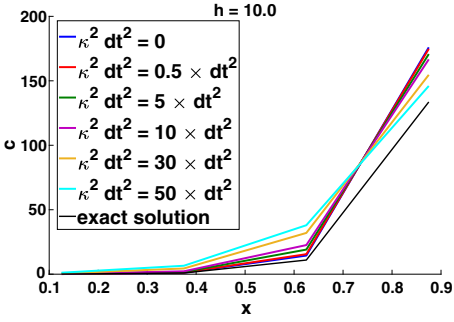

Fig. 3 Comparison of solutions at $T = 3$ with various κ. Here, $\Delta x = 0.25$ and $\tau = 0.001$

affect the accuracy. But it is related to the convexity of the objective function and thus impacts the convergence of our method. Therefore, we try to choose small κ when the convergence problem is not severe.

Example 2 In this numerical example, on the computational region $[0, 1] \times [0, T]$, we consider a nonuniform electric filed $u(x) = -h \sin(\pi x)$, and the initial condition is as follows

$$c^0(x) = \exp(h \sin(\pi x)) + \cos(2\pi x) + h \sin(\pi x), \quad x \in [0, 1].$$

We first let $h = 1.0$ and verify that our scheme can still preserve those physical properties well when dealing with a varying electric field. In Fig. 4, it is observed that the evolution of $c(t, x)$ converges to the equilibrium profile $c^\infty(x)$, the energy dissipates along time to reach the equilibrium state $\mathcal{E}_\infty$, and the total mass in our scheme is maintained well, while the traditional Lagrange Galerkin method cannot preserve the total mass conservation.

Then we let $h = 10.0$. Then the convection term of the NP equation is dominant. A comparison is made between our scheme and the traditional Galerkin method on a coarse grid in space. In Fig. 5, it is seen that the numerical solution values solved with these two methods are all nonnegative. The energy obtained from our scheme quickly reaches the equilibrium state $\mathcal{E}_\infty$, but the energy solved from the Galerkin method appears to increase during a certain period.

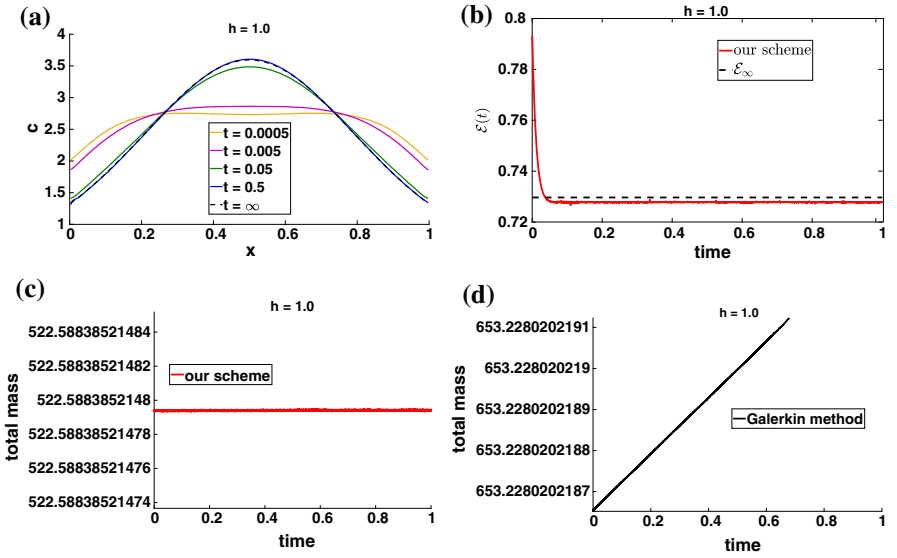

Fig. 4 **a** Evolution of the concentration $c(x, t)$, **b** energy dissipation, **c** total mass calculated with our scheme, and (d) the total mass obtained from the Galerkin method over the time interval $[0, T]$ with $T = 1$, $\Delta x = 0.005$, $\tau = 0.0001$, $\kappa = 0$

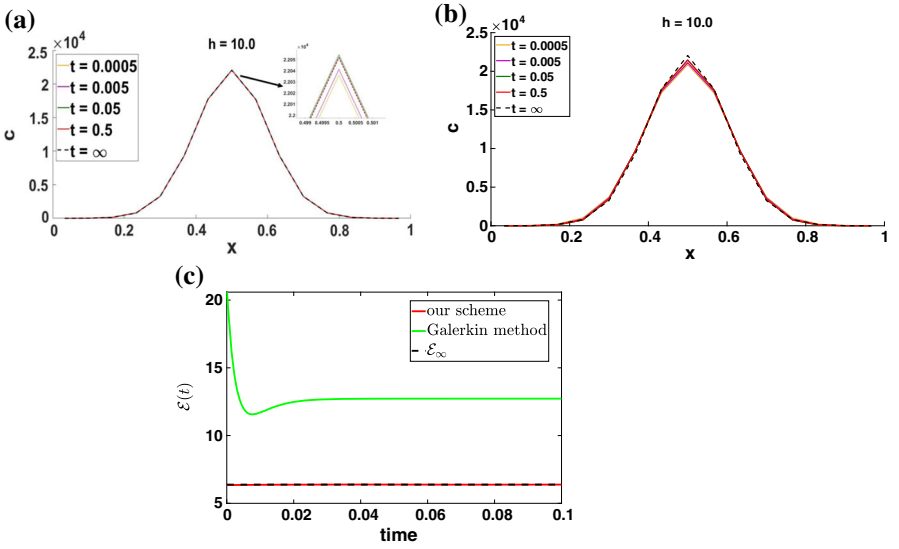

Fig. 5 Evolution of the concentration $c(x, t)$ calculated with **a** our scheme and **b** the classical FEM, **c** energy changing over time of these two methods on the time interval $[0, T]$ with $T = 0.5$, $\Delta x = 0.0667$, $\tau = 0.0001$, $\kappa = 0$

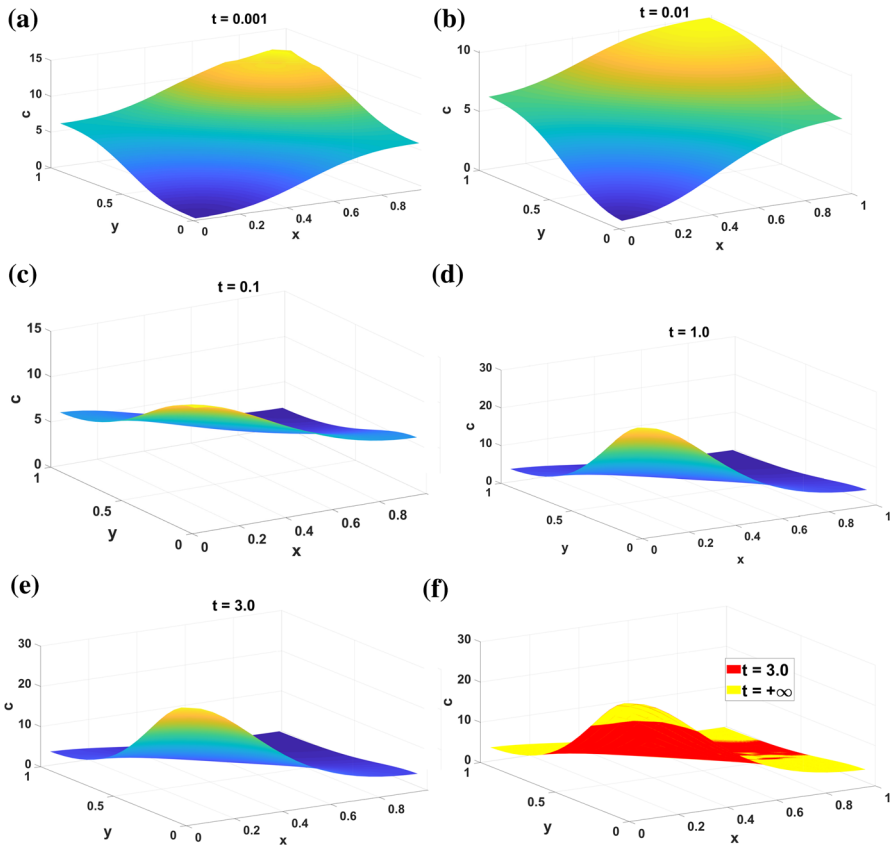

Fig. 6 Evolution of the concentration $c(x, t)$ at different times with $T = 3.0$, $\Delta x = 0.05$, $\tau = 0.001$, $\kappa = 0$

Example 3 In this example, we apply our scheme to a two-dimensional problem on the computational region $[0, 1]^2 \times [0, T]$. The electrical filed $u(x, y) = -\cos(\pi x) - \cos(\pi y)$, and the initial value of the concentration is defined as

$$c^0(x, y) = 2\pi x - \sin(2\pi x) + 2\pi y - \sin(2\pi y), \quad (x, y) \in [0, 1]^2.$$

In Fig. 6, we plot the evolution of the concentration at different times. It is observed that the concentration profiles gradually reach the equilibrium profile c^∞. And in the whole varying process, the concentration is always nonnegative. Figure 7 presents the decay property of the energy and the conservative property of the total mass. This numerical example illustrates that our method can still keep the physical properties of the NP equation well when dealing with a two-dimensional problem.

The above numerical results show that our scheme performs better than the traditional Galerkin method in preserving solution nonnegativity, energy dissipation, and total mass conservation even when the convection term is dominant, and the grid is relatively coarse.

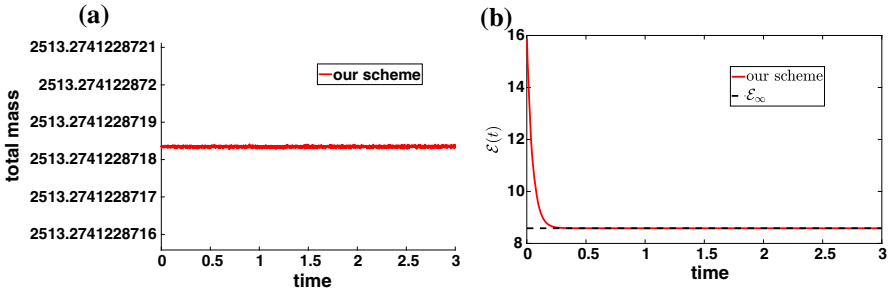

Fig. 7 **a** The total mass conservation and **b** energy dissipation over the time interval $[0, T]$ with $T = 3.0$, $\Delta x = 0.05$, $\tau = 0.001$, $\kappa = 0$

4 Conclusion

In this work, we propose a structure-preserving finite element discretization for the time-dependent NP equation. In our method, we consider the reformulated JKO scheme, which transforms the partial differential equation solution problem into an optimization problem, different from the traditional Galerkin method. If the reformulated JKO scheme is discretized with linear Lagrangian basis functions in space, we find that the obtained discrete objective function is not smooth, and the global convexity of which cannot be proved. Therefore, we introduce the SG approximation technique, and the concentration is discretized with exponential basis functions on each edge of the element. Our discretization strategy and the Fisher information regularization term of the reformulated method guarantee the convexity of the discrete objective function. Furthermore, the additional regularization term can automatically maintain the solution nonnegativity. However, it will also polish the numerical solution and then affect the accuracy, so choosing an appropriate regularization parameter is necessary. In this paper, we prove that our scheme can preserve all physical properties of the NP equation: solution nonnegativity, total mass conservation, and energy dissipation. And these properties are all verified through several numerical experiments. These numerical results also illustrate that our scheme performs better than the traditional Galerkin method with linear Lagrangian basis functions in preserving the physical properties of the NP equation, especially with convection-dominated terms and relatively coarse grids. In the future, we will extend our scheme to solve PNP equations and apply it in real physical system simulations, such as biological ion channel simulations, nanopore simulations, and so on.

Acknowledgements This work was supported by the National Key Research and Development Program of Ministry of Science and Technology under Grant 2016YFB0201304; the China NSF under Grants 11771435 and 22073110; Strategic Priority Research Program of the Chinese Academy of Sciences under Grant XDB36000000; National Natural Science Foundation under Grant 32027801.

References

1. Ambrosio, L., Gigli, N., Savaré, G.: Gradient flows: in metric spaces and in the space of probability measures. Springer, Berlin (2008)
2. Brezzi, F., Marini, L.D., Pietra, P.: Numerical simulation of semiconductor devices. Comput. Methods Appl. Mech. Eng. **75**(1–3), 493–514 (1989)
3. Brunk, M., Kværnø, A.: Positivity preserving discretization of time dependent semiconductor drift-diffusion equations. Appl. Num. Math. **62**(10), 1289–1301 (2012)
4. Buturla, E., Cottrell, P., Grossman, B., Salsburg, K.: Finite-element analysis of semiconductor devices: the fielday program. IBM J. Res. Develop. **25**(4), 218–231 (1981)
5. Cancès, C., Gallouët, T.O., Todeschi, G.: A variational finite volume scheme for Wasserstein gradient flows. Numerische Mathematik **146**(3), 437–480 (2020)
6. Carlen, E.A., Gangbo, W.: Constrained steepest descent in the 2-Wasserstein metric. Annals of mathematics pp. 807–846 (2003)
7. Carlier, G., Poon, C.: On the total variation Wasserstein gradient flow and the tv-jko scheme. ESAIM: Control, Optimisation and Calculus of Variations **25**, 42 (2019)
8. Chow, S.N., Dieci, L., Li, W., Zhou, H.: Entropy dissipation semi-discretization schemes for Fokker-Planck equations. J. Dynam. Diff. Eq. **31**(2), 765–792 (2019)
9. Codina, R.: Comparison of some finite element methods for solving the diffusion-convection-reaction equation. Comput. Methods Appl. Mech. Eng. **156**(1–4), 185–210 (1998)
10. Codina, R., Blasco, J.: Analysis of a stabilized finite element approximation of the transient convection-diffusion-reaction equation using orthogonal subscales. Comput. Visual. Sci. **4**(3), 167–174 (2002)
11. Ding, J., Wang, Z., Zhou, S.: Positivity preserving finite difference methods for Poisson-Nernst-Planck equations with steric interactions: application to slit-shaped nanopore conductance. J. Comput. Phys. **397**, 108864 (2019)
12. Erbar, M.: The heat equation on manifolds as a gradient flow in the Wasserstein space. Annales de l'IHP Probabilités et statistiques **46**, 1–23 (2010)
13. Evans, L.C., Gangbo, W.: Differential equations methods for the monge-kantorovich mass transfer problem (653) (1999)
14. Flavell, A., Machen, M., Eisenberg, B., Kabre, J., Liu, C., Li, X.: A conservative finite difference scheme for Poisson-Nernst-Planck equations. J. Comput. Electron. **13**(1), 235–249 (2014)
15. Gao, H., Sun, P.: A linearized local conservative mixed finite element method for poisson-nernst-planck equations. J. Sci. Comput. **77**(2), 793–817 (2018)
16. Gianazza, U., Savaré, G., Toscani, G.: The Wasserstein gradient flow of the fisher information and the quantum drift-diffusion equation. Arch. Rat. Mech. Anal. **194**(1), 133–220 (2009)
17. He, D., Pan, K.: An energy preserving finite difference scheme for the Poisson-Nernst-Planck system. Appl. Math. Comput. **287**, 214–223 (2016)
18. Hu, J., Huang, X.: A fully discrete positivity-preserving and energy-dissipative finite difference scheme for Poisson–Nernst–Planck equations. Numerische Mathematik pp. 1–39 (2020)
19. John, V., Mitkova, T., Roland, M., Sundmacher, K., Tobiska, L., Voigt, A.: Simulations of population balance systems with one internal coordinate using finite element methods. Chem. Eng. Sci. **64**(4), 733–741 (2009)
20. John, V., Schmeyer, E.: Finite element methods for time-dependent convection-diffusion-reaction equations with small diffusion. Comput. Methods Appl. Mech. Eng. **198**(3–4), 475–494 (2008)
21. Jordan, R., Kinderlehrer, D., Otto, F.: The variational formulation of the Fokker-Planck equation. SIAM J. Math. Anal. **29**(1), 1–17 (1998)
22. Knopp, T., Lube, G., Rapin, G.: Stabilized finite element methods with shock capturing for advection-diffusion problems. Comput. Methods Appl. Mech. Eng. **191**(27–28), 2997–3013 (2002)
23. Li, W.: Transport information geometry i: Riemannian calculus on probability simplex. arXiv preprint arXiv:1803.06360 (2018)
24. Li, W., Lu, J., Wang, L.: Fisher information regularization schemes for Wasserstein gradient flows. J. Comput. Phys. **416**, 109449 (2020)
25. Li, W., Ryu, E.K., Osher, S., Yin, W., Gangbo, W.: A parallel method for earth movers distance. J. Sci. Comput. **75**(1), 182–197 (2018)
26. Li, W., Yin, P., Osher, S.: Computations of optimal transport distance with Fisher information regularization. J. Sci. Comput. **75**(3), 1581–1595 (2018)

27. Liu, C., Wang, C., Wise, S.M., Yue, X., Zhou, S.: A positivity-preserving, energy stable and convergent numerical scheme for the Poisson-Nernst-Planck system. arXiv preprint arXiv:2009.08076 (2020)
28. Liu, H., Maimaitiyiming, W.: Effcient, positive, and energy stable schemes for multi-d Poisson-Nernst-Planck systems. Journal of Scientic Computing **87**(3), 1–36 (2021)
29. Liu, H., Wang, Z.: A free energy satisfying finite difference method for Poisson-Nernst-Planck equations. J. Comput. Phys. **268**, 363–376 (2014)
30. Liu, H., Wang, Z.: A free energy satisfying discontinuous Galerkin method for one-dimensional Poisson-Nernst-Planck systems. J. Comput. Phys. **328**, 413–437 (2017)
31. Liu, H., Wang, Z., Yin, P., Yu, H.: Positivity-preserving third order DG schemes for Poisson–Nernst–Planck equations. arXiv preprint arXiv:2102.00101 (2021)
32. Metti, M.S., Xu, J., Liu, C.: Energetically stable discretizations for charge transport and electrokinetic models. J. Comput. Phys. **306**, 1–18 (2016)
33. Otto, F.: The geometry of dissipative evolution equations: the porous medium equation (2001)
34. Roux, B., Allen, T., Bernche, S., Im, W.: Theoretical and computational models of biological ion channels. Quart. Rev. Biophys. **37**(1), 15 (2004)
35. Scharfetter, D.L., Gummel, H.K.: Large-signal analysis of a silicon read diode oscillator. IEEE Trans. Electron Devices **16**(1), 64–77 (1969)
36. Tu, B., Bai, S., Lu, B., Fang, Q.: Conic shapes have higher sensitivity than cylindrical ones in nanopore DNA sequencing. Sci. Rep. **8**(1), 1–11 (2018)
37. Tu, B., Chen, M., Xie, Y., Zhang, L., Eisenberg, R.S., Lu, B.: A parallel finite element simulator for ion transport through three-dimensional ion channel systems. J. Comput. Chem. **34**(24), 2065–2078 (2013)
38. Tu, B., Xie, Y., Zhang, L., Lu, B.: Stabilized finite element methods to simulate the conductances of ion channels. Comput. Phys. Commun. **188**, 131–139 (2015)
39. Wächter, A., Biegler, L.T.: On the implementation of an interior-point filter line-search algorithm for large-scale nonlinear programming. Math. Program. **106**(1), 25–57 (2006)
40. Wang, Q., Li, H., Zhang, L., Lu, B.: A stabilized finite element method for the Poisson-Nernst-Planck equations in three-dimensional ion channel simulations. Appl. Math. Lett. **111**, 106652 (2021)
41. Xu, J., Lu, B., Zhang, L.: A time-dependent finite element algorithm for simulations of ion current rectification and hysteresis properties of 3D nanopore system. IEEE Trans. Nanotechnol. **17**(3), 513–519 (2018)

Authors and Affiliations

Qianru Zhang[1,2] · Bin Tu[3] · Qiaojun Fang[3,4,5] · Benzhuo Lu[1,2]

✉ Bin Tu
tub@nanoctr.cn

✉ Benzhuo Lu
bzlu@lsec.cc.ac.cn

Qianru Zhang
qrzhang@lsec.cc.ac.cn

Qiaojun Fang
fangqj@nanoctr.cn

[1] State Key Laboratory of Scientific and Engineering Computing, National Center for Mathematics and Interdisciplinary Sciences, Academy of Mathematics and Systems Science, Chinese Academy of Sciences, Beijing 100190, People's Republic of China

[2] School of Mathematical Sciences, University of Chinese Academy of Sciences, Beijing 100049, People's Republic of China

[3] Laboratory of Theoretical and Computational Nanoscience, CAS Key Laboratory of Nanophotonic Materials and Devices, CAS Center for Excellence in Nanoscience, Beijing Key Laboratory of Ambient Particles Health Effects and Prevention Techniques, National Center for Nanoscience and Technology, Chinese Academy of Sciences, Beijing 100190, People's Republic of China

[4] University of Chinese Academy of Sciences, No. 19A Yuquan Road, Beijing 100049, People's Republic of China

[5] Sino-Danish Center for Education and Research, Beijing 101408, People's Republic of China